Supplementary Figures:

Figure S1. Rab11a$^{\Delta IEC}$ intestinal epithelial pathogenesis in postnatal stages.

(A) Villus branching and blunting were detected in postnatal mutant mice.

(B) Immune cells infiltrated into the submucosal and mucosal layers in 5 month old mutant survivors. Immunofluorescent staining for E-Cadherin (green) and pHH3 (red) identified enlarged villi with multiple epithelial cell layers.

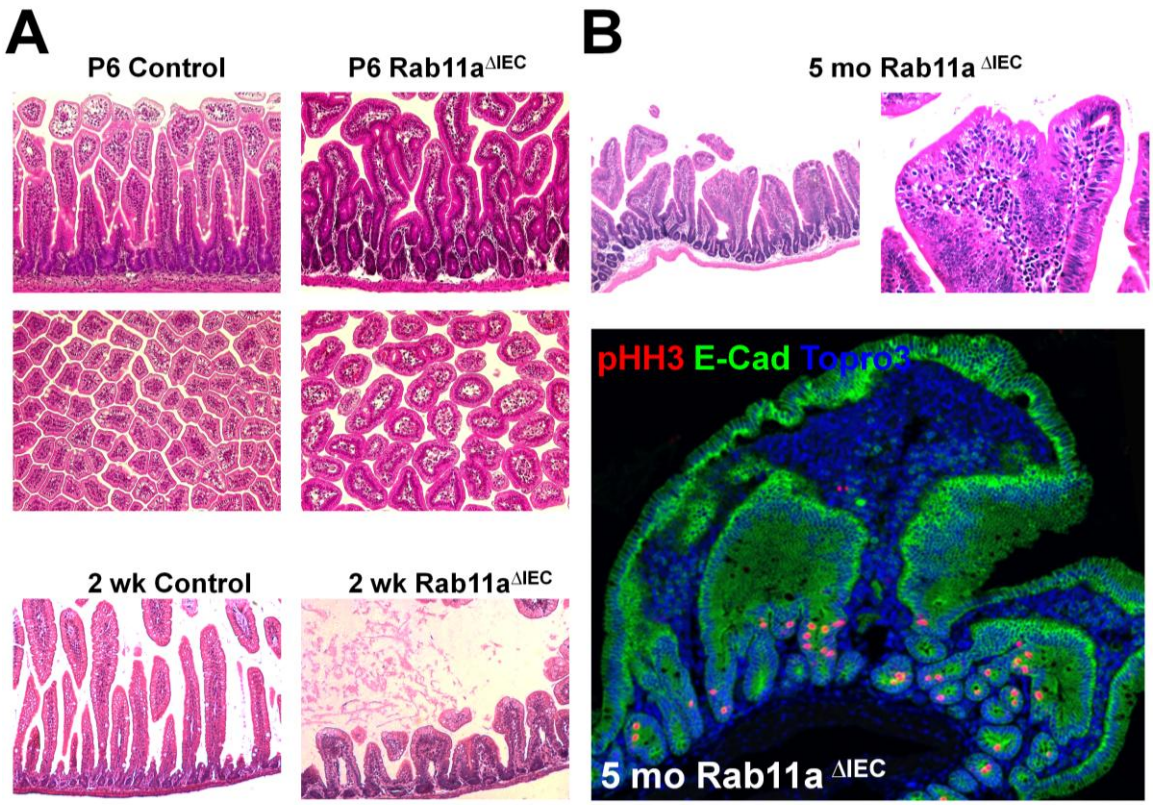

Figure S2. Inducible Rab11a deletion in IECs caused crypt cell proliferation.
Adult Rab11a$^{fl/fl}$; Vil-CreER mice and control littermates Rab11afl/fl were injected with tamoxifen to induce Rab11a deletion. pHH3 staining (green) showed increased mitotic crypt cells in male and female mutant mice.

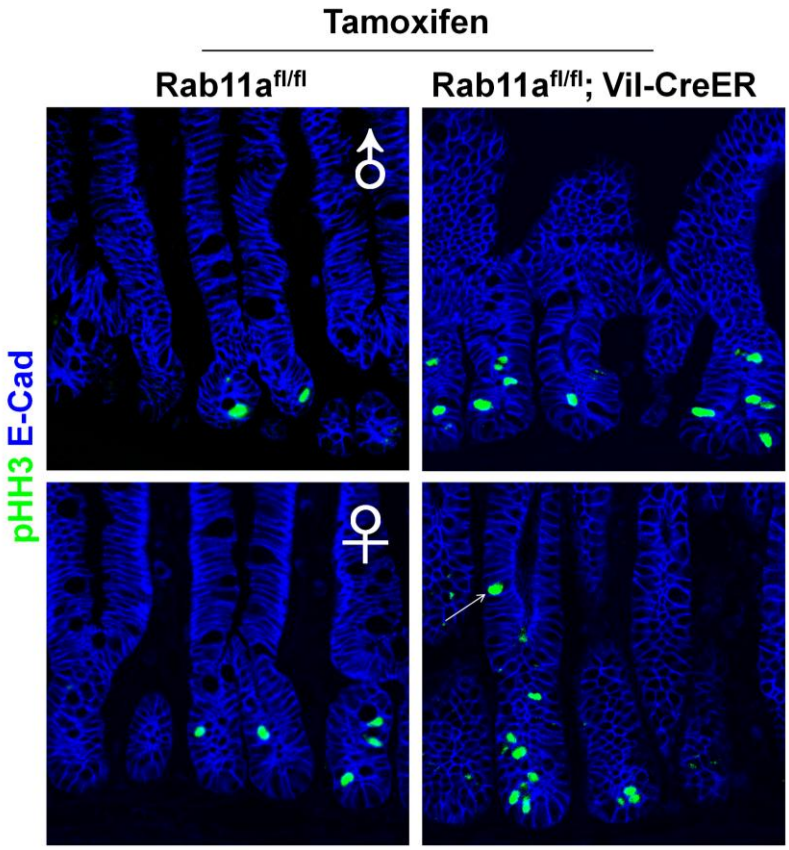

Figure S3. IEC differentiation was not impaired in Rab11a$^{\Delta IEC}$ mice.

(A) Chromogranin A and Lysozyme staining detected enteroendocrine and Paneth cells in mutant intestines.

(B) Transmission EM showed apical microvilli in enterocytes of mutant intestines. White arrows identify apical junctions in mutant epithelia.

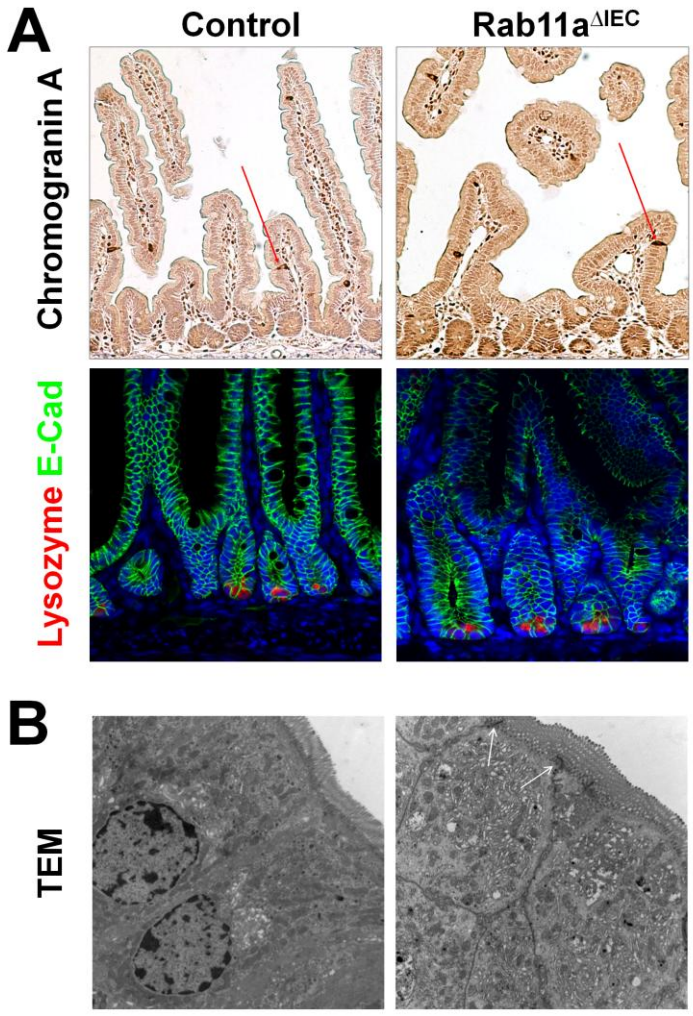

Figure S4. TLR mRNA levels were unchanged in Rab11a-deficient intestines.

(A) Microarray analysis showed no significant change in the expression of a number of TLR genes.

(B) Quantitative RT-PCR showed that TLR9 mRNA levels were unchanged in Rab11a-deficient intestines. $p>0.05$

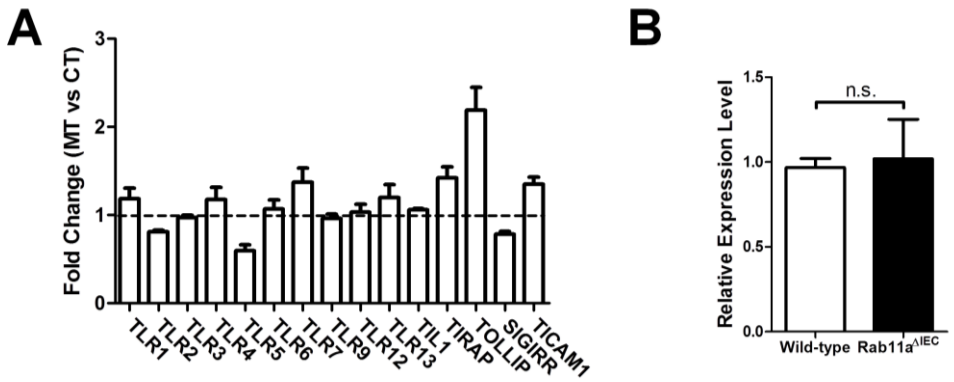

Figure S5. Increased TLR9 aggregations in Rab7^{+} vesicular compartment.

(A) Co-staining for TLR9 (green) and Rab7 (red) showed increased TLR9 aggregates in Rab11a-deficient IECs.

(B) Control and RAB11A knockdown Caco2 cells were treated with CpG, fixed, and co-stained for TLR9 (green) and Rab7 (red). Large TLR9 aggregates that associated to Rab7^{+} vesicles were pointed by arrows in RAB11A depleted cells. Scale bars, 10 μm.

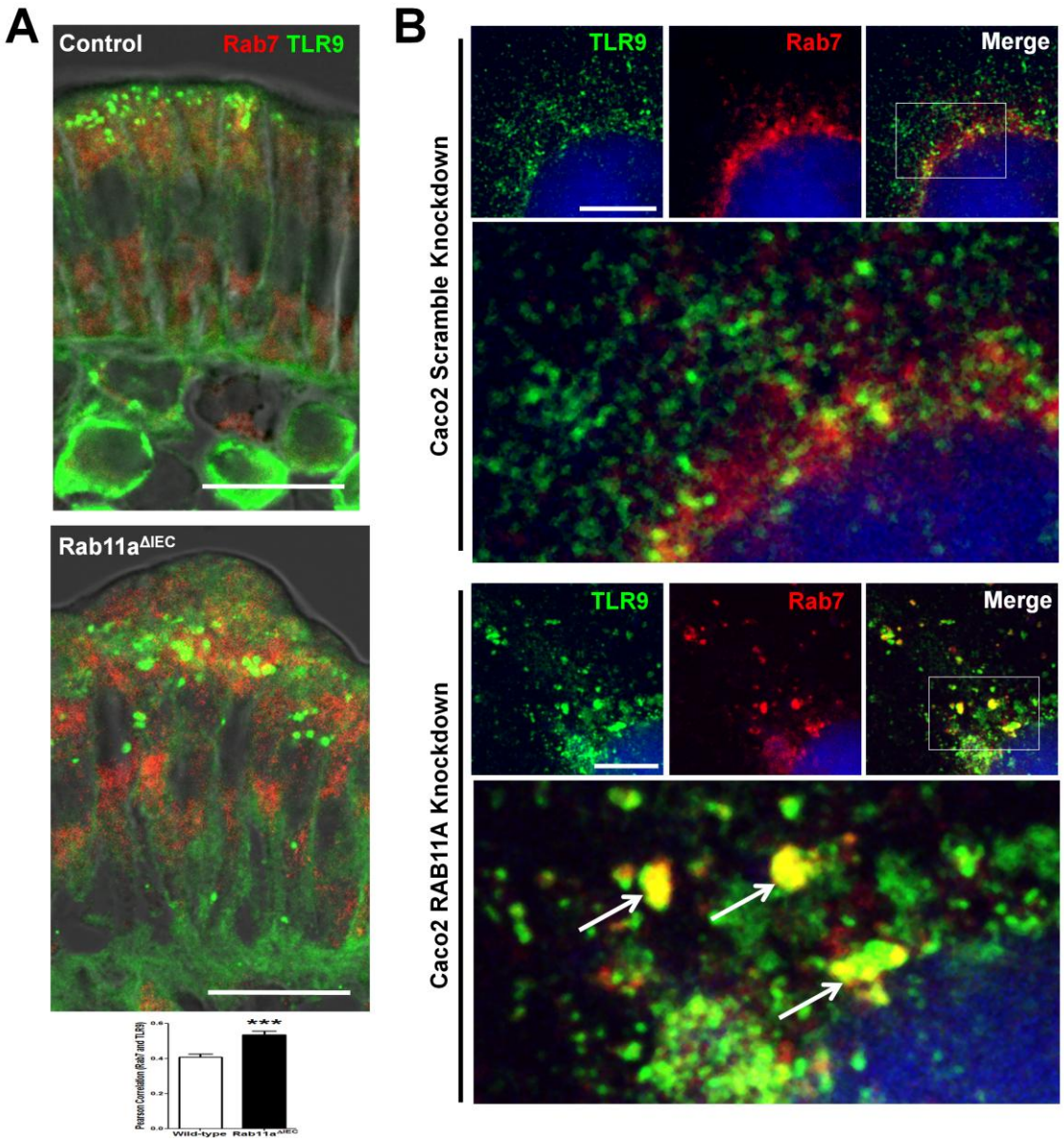

Figure S6. Rab11a deficiency impacts TLR9 fragmentation.

(A) The mouse anti-TLR9 (Imgenex) antibody used in this study detected multiple endogenous TLR9 fragments in human and mouse intestinal lysates (lane 1, 4 and 5), human Burkitt's lymphoma Ramos cell line (lane 2), and human colonic epithelial Caco2 cell line (lane 3). These fragments were diminished in stable TLR9-KD Caco2 cells (lane 4). Note that this antibody does not detect full length TLR9 (arrowhead), which could be detected by the rabbit anti-TLR9 (Cell Signaling) in panel B.

(B) The rabbit anti-TLR9 (Cell Signaling #5845, human TLR9-specific) antibody detected full-length receptor in Ramos and human monocytic THP1 cells (lane 1 and 4), but not in Caco2 cells. The ~50-kDa product seen in both Ramos and Caco2 cells (lane 1 and 3) was diminished in stable TLR9-KD Caco2 cells (lane 2).

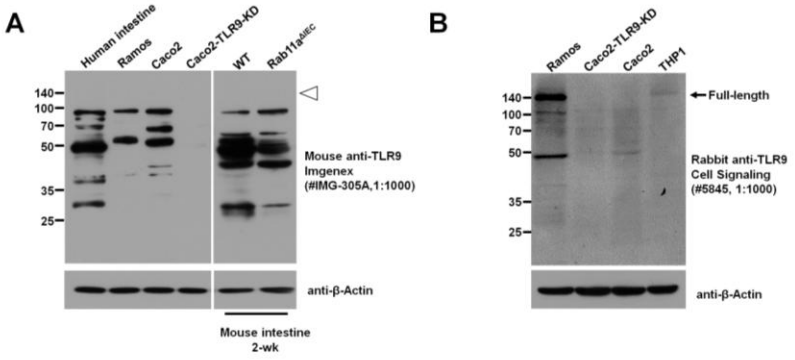

Figure S7. Rab11a deficiency alters TLR9 intracellular traffic in cultured cells.

(A) Co-IP analyses showed that both the 95 and 55 kDa TLR9 fragments were contained in RAB11A vesicular compartments (lane 3).

(B) Transient knockdown of RAB11A in Caco2 or treating the cells with Monensin changed TLR9 fragment pattern (see arrowhead). Compare lane 1 to lane 2 & 3.

(C) Isolation of surface proteins following biotinylation detected 30% reduction of TLR9 localization at RAB11A-KD Caco2 cell surface (compare lane 2 with lane 1). Note that only the 95 kDa TLR9 fragment could be biotinylated (see arrowhead).

(D) Reciprocal co-IP between TLR9 and RAB7 showed increased TLR9 in RAB7+ compartments (arrowheads). Compare lane 2 to lane 1. Note the strong bands appearing at 50-kDa in the co-IP lanes (1 and 2) corresponded to antibody heavy chain.

(E) Caco2 cells were lysated in 0.1% NP-40, 50 mM Tris-HCl pH 7.5, 150 mM NaCl on ice for 30 minutes. Supernatants were collected after centrifugation and loaded on poly-lysine coated glass for microscopic analysis. DIC micrograph showed the largely preserved vacuolar/vesicular structures, suggesting that the lipid bilayer remained intact under these conditions, and that membrane proteins were unlikely to be completely solubilized, consistent with previous reports (Schuck et al, 2003; Yu et al, 2008).

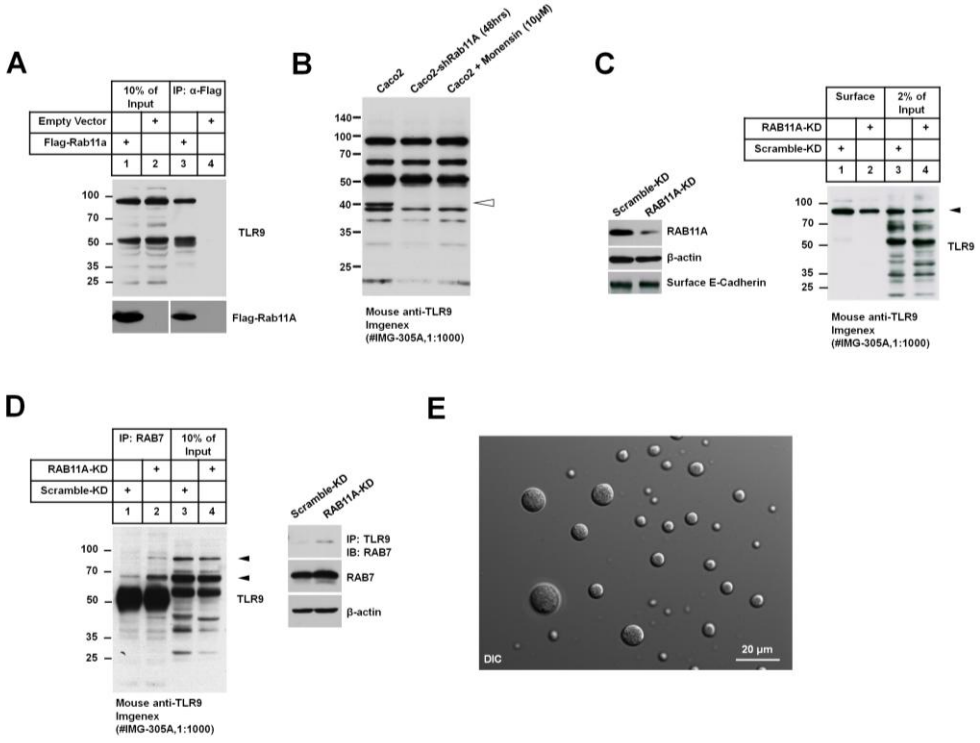

Table S1: Primers for Quantitative RT-PCR.

	Forward (5'-3')	Reverse (5'-3')
IL1β	CCTTGGGCCTCAAAGGAAAG	TCTTCTTCTTTGGGTATTGCTTGG
IL6	CAAAGCCAGAGTCCTTCAGAGA	GCATTGGAAATTGGGGTAGG
IL1F8	GTTGAGATGGAGGGCAAACC	GGAGCCCTCTATGCCATGAT
LYZ1	GGTGGTGAGAGATCCCCAAG	CAGACTCCGCAGTTCCGAAT
CXCL1	GACCCTGAAGCTCCCTTGGT	GAAGCCAGCGTTCACCAGAC
CXCL5	CCAGAAGGAGGTCTGTCTGGAT	TGCGAGTGCATTCCGCTTAG
LGR5	TGAGCGGGACCTTGAAGATT	AGGTGCTCACAGGGCTTGAA
ASCL2	TCCAGTTGGTTAGGGGGCTA	GCATAGGCCCAGGTTTCTTG
OLFM4	CTCTTTTCCACCAGCACACG	TAAACCCCAGCCAGTTGAGC
BMI1	GAGCAGATTGGATCGGAAAG	GCATCACAGTCATTGCTGCT
CTSL	ACCATGGGGTTCTGTTGGTG	AGCCTTCCATACCCCATTCA
CIAP2	GGGAAATTGACCCTGCGTTA	TTTCCGCAACTGTTCTTCCA
TLR9	CGGGAGAATCCTCCATCTCC	TACCCAGGGCCAGAGTCTCA
β-Actin	TTGCTGACAGGATGCAGAAG	CCACCGATCCACACAGAGTA

Supplementary Experimental Procedures:

Antibodies and Reagents

The sources of antibodies, proteins, and inhibitors are as follows: mouse anti-Rab11a (BD Transduction Laboratories, #610656), rabbit anti-Rab11a (US Biological, R0009), rat anti-BrdU (Accurate Chemicals, OBT0030G), mouse anti-E-Cadherin (BD Transduction Laboratories, #610181), rabbit anti-phosphorylated histone H3 (Millipore, MABE13), rat anti-BrdU (AbD Serotec, OBT0030G), goat anti-GFP (Abcam, ab6673), rabbit anti-chromogranin A (Immunostar, #20085), rabbit anti-Lyz (Biogenex, AR024-5R), alkaline phosphatase kit (Vector Laboratories, SK-5100), rat anti-F4/80 (AbD Serotec, MCA497GA), goat anti-IL6 (R&D systems, AF-406-NA), mouse IL6 (Cell Signaling, #6514), rabbit anti-phosphorylated p38 MAPK (Cell Signaling, #4511), rabbit anti-p38 MAPK (Cell Signaling, #8690), rabbit anti-phosphorylated JNK (Cell Signaling, #4668), rabbit anti-JNK (Cell Signaling, #9258), rabbit anti-phosphorylated Stat3 (Cell Signaling, #9145), mouse anti-Stat3 (Cell Signaling, #9139), rabbit anti-P65 (Cell Signaling, #8242), rabbit anti-RelB (Cell Signaling, #4922), rabbit anti-Villin (Santa Cruz, sc-7672), rabbit anti-lamin A/C (Santa Cruz, sc-20681), mouse anti-β-Actin (Santa Cruz, sc-8432), rabbit anti-β-Catenin (Abcam, ab32572), mouse anti-TLR9 (Imgenex, IMG-305A), rabbit anti-TLR9 (Cell Signaling, #5845), rabbit anti-Rab7 (Cell Signaling, #9367), rabbit anti-MyD88 (Cell Signaling, #4283), rabbit anti-phosphorylated IKKα/β (Cell Signaling, #2697), rabbit anti-phosphorylated ERK (Cell Signaling, #3470), anti-LAMP2 (Developmental Studies Hybridoma Bank, ABL-93), TO-PRO-3 (Invitrogen, T3605), BAY11-0782 (Santa Cruz, sc-200615). Human small intestinal tissue lysate (Catalog No. NBP2-25033) and human Burkitt's lymphoma Ramos whole cell lysate (Catalog No. NBP2-10264) were purchased from Novus Biologicals.

Mice

All mice were maintained in alternating 12-hour light/dark cycles on a regular diet at Rutgers Animal Facility in Newark. To stage the embryos, vaginal plug was check for female mice every morning after mating setup. The morning of plug detection was designated as E0.5. Experimental procedures were approved by the Rutgers Institutional Animal Care and Use Committee. For inducible Rab11a ablation, mice were

intraperitoneally injected with tamoxifen (1mg/mouse, Sigma-Aldrich, #T5648) dissolved in corn oil (Sigma-Aldrich, #C8267) and pre-warmed to 37℃. Mice were sacrificed 7 days after injection.

Cell Culture, Plasmid, and Surface Protein Isolation

Human monocytic THP1 cells were purchased from ATCC and maintained in RPMI1640 supplemented with 10% fetal bovine serum, 0.05 mM 2-mercaptoethanol, 100 IU/ml penicillin and 10 μg/ml streptomycin at 37 °C. The human colorectal cancer cell line Caco2 and RAB11A-KD Caco2 cells were maintained in RPMI1640 medium supplemented with 10% fetal calf serum (FCS), 8 U/ml insulin, 0.5 mg/ml hydrocortisone, 10 μg/ml thioglycerol, and 1% penicillin and streptomycin or in MEM medium supplemented with 20% fetal bovine serum (Sigma) and 1% penicillin and streptomycin at 37 ℃, in 5% CO_2. Of note, ATCC states that this cell line expressed heat stable enterotoxin (Sta, *E. coli*).

To establish Caco2-shTLR9 KD stable cell line, Caco2 cells were infected with lentiviral shTLR9 particles for 8 hrs in MEM containing 1 μg/ml polybrene at 37 °C and selected by 5 μg/ml puromycin for 5 days. Packaging of lentiviral shTLR9 particles followed the TRC lentiviral packaging protocol provided by Broad Institue (http://www.broadinstitute.org/rnai/public/resources/protocols). Briefly, human TLR9 specific shRNA vector (Sigma, TRCN0000358885) was co-transfected into 293T cells with psPAX2 and pMD2.G (Addgene). After 48 hrs of culture, lentiviruses in culture medium were pelleted via ultracentrifugation at 30,000g for 2 hrs and resuspended in MEM.

Human Rab11a tagged with the amino-terminal Flag epitope was cloned into pQCXIP vector for overexpression in LIM2550 cells. Stable knockdown of RAB11A in Caco2 cells was achieved using a Lentiviral knockdown system (Sigma)(Gao & Kaestner, 2010). To produce cysts, Caco2 and Caco2-Rab11AKD were trypsinized, mixed with Matrigel and plated into each well of a chambered slide. After solidification, cells were overlayed with culture medium and allowed to grow for 5 days.

Plasma membrane (PM)-bound protein extraction was performed using Cell Surface Protein Isolation Kit (Pierce, #89881) according to the manufacture's manual.

Confluent Caco2 and RAB11AKD Caco2 cells grown in 10-cm dish were incubated with 0.5 mg/ml EZ-Link sulfo-NHS-LC-biotin in cold PBS for 30 mins. After termination of biotinylation reaction, the cells were washed, scraped into cell lysis buffer containing protease inhibitor, and disrupted by sonication. After centrifugation, supernatant was incubated with NeutrAvidin agarose for 4 hrs at 4℃. After 2 washes, 1x SDS sample buffer was used to elute proteins from agorose for Western blot analysis. All Western blots were repeated multiple times.

EdU/BrdU Labeling and Detection, Immunofluorescent Analysis

For in vivo labeling, mice were intraperitoneally injected with EdU labeling reagent (0.1 mM/kg body weight, Invitrogen, A10044) dissolved in sterile PBS or BrdU labeling reagent (10 ml/kg body weight, Invitrogen, #00-0103). After 30 minutes, mice were sacrificed and intestine harvested for fixation. For in vitro labeling, organoids were kept in crypt culture medium containing 10 μM EdU for 30 to 60 mins before fixation. EdU detection was performed using Click-iT EdU Alexa Fluor 555 imaging kit according to the manufacture's manual (Invitrogen, #10338). Cells with positive EdU/BrdU labeling within a single crypt or organoid were counted for a total number that was reported in the graph. Procedures for immunohistochemistry and immunofluorescent analyses have been described(Sakamori et al, 2012).

Multiplex Cytokine ELISA

Cytokines and chemokines in the supernatant of organoid culture medium were measured by an ELISA kit (SABiosciences, MEM-008A or Pierce, EM2IL6) according to the manufacture's instruction with some modifications. Briefly, 500 to 800 crypts per well were seeded into a 24-well plate and cultured with organoid culture medium. Medium was replenished every day. After 6 days of culture, 100 μl of cell culture media were added into each well of ELISA plate in duplicate and incubated at room temperature for 2 hrs. After 3 times of wash, 100 μl of detection antibodies and diluted streptavidin-HRP were sequentially applied and incubated in dark for 2 hrs and 30 mins, respectively. 100 μl of development solution was then added after 3 washes, followed by an incubation of 30 mins in dark prior to termination with stop solution. The ELISA plate was then read at

OD450 nm by a Glomax Multi-Detection System (Promega). Experiments were repeated for 2 to 6 times for different conditions.

Multiplex cytokine assay for mouse serum was conducted using Milliplex MAP kits (Millipore, MCYTOMAG-70K). Serum samples were collected from control and Rab11a$^{\Delta IEC}$ mice via retro orbital sinus. 25 μL mouse serum was then mixed with antibody-immobilized magnetic beads and incubated with agitation overnight at 4 ℃. After 2 washes, detection antibodies and streptavidin-phycoerythrin were sequentially added and incubated for 1 hr and 30 mins, respectively. Beads were then suspended in sheath fluid and analyzed by MAGPIX with xPONENT software.

Microarray Analysis and qRT-PCR

For microarray analysis, 6 pairs of Rab11$^{\Delta IEC}$ and littermate control mice (P3) were sacrificed and small intestine tissue harvested for RNA extraction using RNeasy mini Kit (Qiagen, #74104). After RNA quality control, 4 pairs of total RNA (250 ng) with satisfactory quality were amplified and labeled for hybridization. The procedure of microarray hybridization and data processing has been previously described (Gao & Kaestner, 2010). qRT-PCR was performed as previously described(Sakamori et al, 2012). Specific primers are listed in **Table S1**. A two-color heat map was created using Cluster version 3.0 (http://bonsai.hgc.jp/~mdehoon/software/cluster/software.htm) and JAVA TreeView version 1.1.6r4 (http://sourceforge.net/projects/jtreeview/files/) with green/red color scale on a $\log_2$ basis. NIH DAVID analysis was performed to obtain enrichment scores for different gene categories.

Intestinal Barrier Function Assay

Procedures for intestinal barrier function tests were essentially the same as described(Roche et al, 2010) with some modifications. Briefly, 5-cm segments of the duodenum and ileum taken from two pairs of 5-month old female control and Rab11a$^{\Delta IEC}$ mice were individually everted and prepared as sacs or sleeves. The everted gut sacs were filled with Krebs ringer buffer (KRB), tied at both extremities and immersed into pre-warmed KRB containing 0.2 μM ^{3}H-L-glucose and 20μM ^{14}C-inulin. After 10 mins of incubation with continuous aeration with 95% O_2/5% CO_2 at 37 ℃, gut sacs were rinsed

with cold KRB, dried and opened. The radioactivities of ^{3}H-L-glucose and ^{14}C-inulin in 50 μl of the fluid from inside and outside of the gut sacs were determined in duplicate by dual-label counting with a manually calibrated LS 6500 Liquid Scintillation Counter (Beckman Coulter, Fullerton, CA). The active accumulation of radioactive molecules in the inside fluid was expressed as a ratio of the final quantity of ^{3}H-L-glucose or ^{14}C-inulin inside/outside.

Co-immunoprecipitation (Co-IP) Analyses

Intestinal tissues or Caco2 cells were homogenized in cold lysis buffer: 50 mM Tris-HCl pH 7.5, 150 mM NaCl, 0.5% NP-40 (0.1% for cell lysis), 1 mM $NaVO_4$, 2 ×protease inhibitor cocktail, and 1×phosphotase inhibitor cocktail. Note that at these concentrations, the non-ionic detergent used was not expected to solubilize the majority of membrane proteins (Schuck et al, 2003; Yu et al, 2008), in particular with the fact that Rabs including Rab11a resisted 1% Triton X-100 extraction (3 hrs, 4℃) by retaining in the detergent-resistant membrane fractions (Yu et al, 2008). To monitor and verify that the lysis procedures preserved intracellular membrane compartments without markedly solubilizing membrane compartments, we collected lysate supernatant following a centrifugation at 5,000 g for 10 minutes, applied onto poly-lysine coated glass slides, and examined membrane integrity under microscope. Consistent with previous reports (Yu et al, 2008), vacuolar/vesicular structures with heterogeneous sizes maintained their integrity suggesting that the lipid bilayer remained intact under these conditions and that most membrane proteins were unlikely to be solubilized **(Fig. S7E)**. Intestinal tissue lysates (2 mg) or cell lysates (1 mg) were then incubated with specific antibodies that were conjugated to the protein A/G agarose beads (Santa Cruz, sc-2003) at 4 ℃ for 4 hrs. After washes, beads were suspended in 40 μl of 1 × SDS sample buffer, denatured at 95 ℃ for 10 min and resolved on 10% SDS-PAGE. Procedures for Western blot were described previously(Sakamori et al, 2012). Experiments were repeated for at least 3 times using different tissue samples.

Transmission Electron Microscopy (TEM)

TEM analyses for mouse intestinal tissues have been described previously (Gao & Kaestner, 2010). Intestinal tissues were dissected, minsed into 1 to 2 mm^2 pieces, and immediately immersed into fixative buffer (2% paraformaldehyde, 2.5% glutaraldehyde in 0.1M sodium cacodylate, pH 7.4) for overnight fixation at 4℃. After 2 washes in sodium cacodylate, samples were post-fixed in 2.0% osmium tetroxide for one hour, dehydrated, and processed for analyses.

References:

Gao N, Kaestner KH (2010) Cdx2 regulates endo-lysosomal function and epithelial cell polarity. *Genes & development* **24**(12)**:** 1295-1305

Roche M, Neti PV, Kemp FW, Agrawal A, Attanasio A, Douard V, Muduli A, Azzam EI, Norkus E, Brimacombe M, Howell RW, Ferraris RP (2010) Radiation-induced reductions in transporter mRNA levels parallel reductions in intestinal sugar transport. *American journal of physiology Regulatory, integrative and comparative physiology* **298**(1)**:** R173-182

Sakamori R, Das S, Yu S, Feng S, Stypulkowski E, Guan Y, Douard V, Tang W, Ferraris RP, Harada A, Brakebusch C, Guo W, Gao N (2012) Cdc42 and Rab8a are critical for intestinal stem cell division, survival, and differentiation in mice. *The Journal of clinical investigation* **122**(3)**:** 1052-1065

Schuck S, Honsho M, Ekroos K, Shevchenko A, Simons K (2003) Resistance of cell membranes to different detergents. *Proc Natl Acad Sci U S A* **100**(10)**:** 5795-5800

Yu MJ, Pisitkun T, Wang G, Aranda JF, Gonzales PA, Tchapyjnikov D, Shen RF, Alonso MA, Knepper MA (2008) Large-scale quantitative LC-MS/MS analysis of detergent-resistant membrane proteins from rat renal collecting duct. *American journal of physiology Cell physiology* **295**(3)**:** C661-678